Available online at www.sciencedirect.com
SCIENCE DIRECT®
International Journal of Mass Spectrometry 231 (2004) 147–155
International Journal of Mass Spectrometry
www.elsevier.com/locate/ijms

Gas chromatography–electron ionization mass spectrometry and liquid chromatography–electrospray tandem mass spectrometry for determination of impurities in the anti-cancer drug isophosphoramide mustard

Richard B. Cole [a,*], Chau-Wen Chou [a], Stephen M. Boué [b], Blaise W. LeBlanc [c], Andrew H. Rodgers [c], Robert F. Struck [d], Lee Roy Morgan [c]

[a] *Department of Chemistry, University of New Orleans, 2000 Lakeshore Drive, 102 Chemical Sciences Bldg., New Orleans, LA 70148, USA*
[b] *Southern Regional Research Center, USDA, ARS, 1100 Robert E. Lee Blvd., New Orleans, LA 70179, USA*
[c] *DEKK-TEC Inc., 4200 Canal St., Suite A, New Orleans, LA 70119, USA*
[d] *Biochemistry and Molecular Biology Department, Southern Research Institute, Birmingham, AL 35205, USA*

Received 18 July 2003; accepted 6 October 2003

Dedicated to Professor Jean-Claude Tabet in celebration of his 60th birthday

Abstract

Isophosphoramide mustard (IPM) is known to have substantial anti-cancer activities in various animal models. Liquid chromatography–electrospray mass spectrometry (LC–ES–MS) and LC–ES–MS/MS methodologies have been developed and applied to the analysis of synthesized preparations of IPM. Our studies reveal that the principal impurity in IPM is *N*-(2-chloroethyl)-*N′*-ethylphosphorodiamidic acid (MC-IPM) formed by dehydrochlorination of IPM with subsequent hydrogenation during synthesis. This impurity is present at levels in the range of 2–5% depending upon synthesis conditions. In addition, a second IPM derivative has been characterized by LC–ES–MS/MS and has been shown to be the product of a reaction of IPM with the dilute perchloric acid mobile phase used for liquid chromatography separations. The LC–ES–MS/MS method has been successfully employed to detect IPM spiked into a blood plasma sample. This work establishes that LC–ES–MS/MS is a viable tool for the detailed characterization of IPM and related products.

Keywords: LC–ES–MS/MS; IPM; Perchloric acid; Isophosphoramide mustard; Mass spectrometry

1. Introduction

Isophosphoramide mustard (IPM), a metabolite of ifosfamide, is being readied for clinical trials [1–12]. Studies with IPM suggest that the agent has improved anticancer activities in standard animal models, when compared to phosphoramide mustard (PM) and other mustards, ifosfamide and cyclophosphamide (CPA) [9,12]. The structures of these anti-cancer compounds are given in Fig. 1. Biochemical studies suggest that IPM does not alkylate as a typical nitrogen mustard but rather as a phosphorodiamidate anion and may cross-link DNA differently from that of classical nitrogen and phosphoramide mustards [5,9,11]. As expected, the toxicities of IPM are different from those of ifosfamide and CPA [2–4,12].

While the pharmacokinetics of CPA and PM have been well investigated, few reports on the pharmacokinetics of IPM have appeared in the literature [6–8]. Similar to PM, IPM has hydrolytic pathways that apparently follow first-order kinetics; at 38 °C the half-life of IPM was 45 min in aqueous phosphate buffer of pH 7.4, while at pH 1.7 the half-life increased to 128 min [9]. In rat plasma, the half-life was 13 min after an initial dose of 40 mg/kg [9].

It is well documented that for phosphamides, P–N hydrolysis is more probable at low pH (e.g., below 2), while nucleophilic displacement of the amide moiety by a hydroxyl anion can occur at higher pH values [9]. In contrast, phosphorus amides are more susceptible to X–N cleavage at

* Corresponding author. Tel.: +1-504-280-6311; fax: +1-504-280-6860.
E-mail address: rcole@uno.edu (R.B. Cole).

1387-3806/$ – see front matter © 2003 Elsevier B.V. All rights reserved.
doi:10.1016/j.ijms.2003.10.013

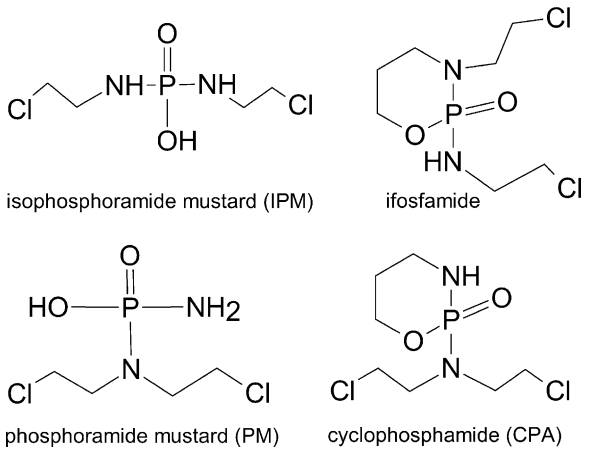

Fig. 1. Structures of IPM and related anti-cancer compounds.

lower pH values than are carbonyl amides, and at least three possible mechanisms can account for the cleavage [11].

Pharmacokinetic studies in mice, dogs and monkeys predict an acceptable starting dose for humans of 30 mg/m^2 with a clearance of 40.5 l/h, a $T_{1/2\alpha}$ of 10 min and a $T_{1/2\beta}$ of 1.75 h for a 70 kg human [12]. This paper attempts to complete the profile for possible IPM degradation products that could occur. The data will be used to document potential routes for IPM disposition in vivo.

2. Experimental

2.1. Chemicals

All employed chemicals (other than IPM) and solvents (except for HPLC-grade water that was obtained from EM Science (Gibbstown, NJ)) were purchased from Aldrich (Milwaukee, WI).

2.2. Synthesis and derivatization of IPM

The synthesis of IPM was based on the procedure developed by Struck et al. [1]. Due to the known instability of IPM to moisture, it was stored at −20 °C in the presence of a desiccant. Prior to analyses, fresh samples were thawed and prepared in the designated solvent systems (see below). IPM dissolves readily in DMF.

2.3. Gas chromatography–mass spectrometry (GC–MS)

For all GC–MS analyses, the derivatization technique developed by Mawhinney et al. [10] was used. Briefly, 100 μl of the sample solution and 50 μl of *t*-butyldimethylsilyl-*N*-methyltrifluoroacetamide (TBDMS) were mixed in an air-tight, crimp-sealed vial (Fisher Scientific, Houston, TX). The mixture was heated at 70 °C for 5 min and then allowed to stand for 2 h at room temperature. The derivatization yield is expected to be approximately 90% (G. Bastian, personal communication). Two microliters of the mixture was injected into a gas chromatograph (Fisons, Model GC 8060, UK) coupled to a mass spectrometer (Micromass Quattro II, Cheshire, UK) equipped with an electron ionization (EI) source. The capillary column (HP-1MS, 30 m long × 0.32 mm i.d. × 0.25 μm film thickness) was purchased from Agilent (Palo Alto, CA). Helium gas was the carrier gas with the instrument pressure regulator set at 47 kPa corresponding to a flow rate of approximately 20 ml/min. The initial oven temperature was 180 °C. After the injection, the temperature was maintained at 180 °C for 2 min, and then was raised at a rate of 8 °C/min to 200 °C. The temperature was maintained at 200 °C for 2 min, and then raised to 250 °C at the rate of 6 °C/min and allowed to remain at 250 °C for 2 min before cooling down to the starting condition. The derivatization product corresponding to IPM yields a fragment ion at *m/z* 355 in the EI mass spectrum, with a typical retention time of about 7 min. The electron energy, emission current, and repeller were set at 70 eV, 231 μA, and 7.2 V, respectively. The source temperature was 200 °C.

2.4. High performance liquid chromatography

Direct high performance liquid chromatography (HPLC) determinations were carried out at DEKK-TEC, using a Pharmacia Liquid Chromatograph (Piscataway, NJ) equipped with an ODC C-18 reversed phase column (Alltech, Deerfield, IL). The dimensions of the column were 25 mm × 4.1 mm (i.d.) and the packing particle size was 10 μm. The HPLC system was operated isocratically at a flow rate of 3.0 ml/min. The mobile phase was prepared as 0.005 M perchloric acid (Aldrich, Milwaukee, WI) in HPLC-grade water to give pH 2.1 [6]. The detector was set at 206 nm for the detection of intact IPM and possible impurities. IPM was dissolved in the mobile phase prior to LC analysis. The concentration of the stock solution was 8.0 μg/μl; ∼20 μl of sample was injected.

2.5. On-line liquid chromatography-mass spectrometry (LC–MS) and LC–MS/MS

Liquid chromatography–electrospray tandem mass spectrometry analyses were performed using the same Micromass Quattro II mass spectrometer described above. A programmable syringe pump (ISCO, Model 100 D, Lincoln, NE) equipped with a microbore ODC—Wakosil II 5C-18 RS HPLC reversed-phase column (dimension 150 mm × 1 mm, particle size 5 μm) from SGE (SGE, Austin, TX) was used for all analyses. The same mobile phase described in the HPLC-UV assay was used for LC–MS. The stock solution of IPM was again at a concentration of 8.0 μg/μl (except for quantitative studies) dissolved in the mobile phase. The optimum flow rate for LC–MS analysis was 35 μl/min. The eluent from the LC column was introduced directly into the mass spectrometer without splitting. ES–MS was operated in the positive ion mode using nitrogen as both the nebulizing

and the drying gas with flow rates of 15 and 350 l/h, respectively. The source temperature was set at 120 °C. The ES needle voltage was held at 2.81 kV; while the cone voltage was set at 46 V to minimize the appearance of water clusters. During all MS analyses, the vacuum was maintained at $\sim 1 \times 10^{-5}$ mbar. For MS/MS analyses employing collision-induced decomposition (CID), the collision gas cell pressure was adjusted to 3.3×10^{-4} mbar (gauge external to the cell), while the collision energy was set at 30 eV. Prior to LC–MS/MS analyses, a test run of LC–MS was conducted (60 min to ensure total elution) to detect all ions in the *m/z* range of 50–450. In a subsequent run, LC–MS/MS was performed on selected ions observed in the LC–MS run.

3. Results and discussion

Due to the instability of IPM in aqueous solutions, analyses of water-based samples can be problematic. Determination of IPM and related products was first performed by GC–MS. For chromatographic analyses, of course, a large advantage afforded by mass spectrometric detection is that structural information may be deduced for individual eluting species, e.g., in these studies, by-products formed during synthesis, and in future studies, metabolites.

3.1. GC–MS analysis

Because of the thermal lability of IPM, GC–MS analyses require a derivatization step. Fig. 2a shows the total ion chromatogram (TIC) resulting from a 2.0 μl injection of ∼10 ng/μl (=∼20 ng) of the product of *t*-butyldimethylsilyl-*N*-methyltrifluoroacetamide derivatization. The initial descent of the TIC corresponds to the tailing portion of the injected solvent. The latter portion of the TIC is magnified by a factor of 30. In this magnified section, the peak corresponding to the main product appears at 6.87 min. This doubly derivatized IPM molecule yields only fragments in the EI mass spectrum, i.e., $M^{+\bullet}$ is not visible. The selected ion chromatogram of the principal fragment at *m/z* 355 appears in Fig. 2b. Fig. 2c shows the EI mass spectrum averaged across the entire width of the peak eluting at 6.87 min. A blank injection produced the EI spectrum shown in Fig. 2d indicating a substantial background of phthalate esters (from plasticizers, yielding *m/z* 149) and background from column bleed (e.g., *m/z* 207, 281, and 355). This last peak at *m/z* 355 (note absence of M + 2 peak in Fig. 2d) originating from elution of the stationary phase was observed to some degree from all employed dimethylpolysiloxane columns, even the so-called "low bleed" variety. Because the principal fragment of the IPM derivative used for quantitation appears at *m/z* 355, the presence of this background peak is particularly troublesome. Its presence held the lower limit of GC–MS detection to about 1.0 ng, or 0.5 ng/μl employing injections of 2.0 μl.

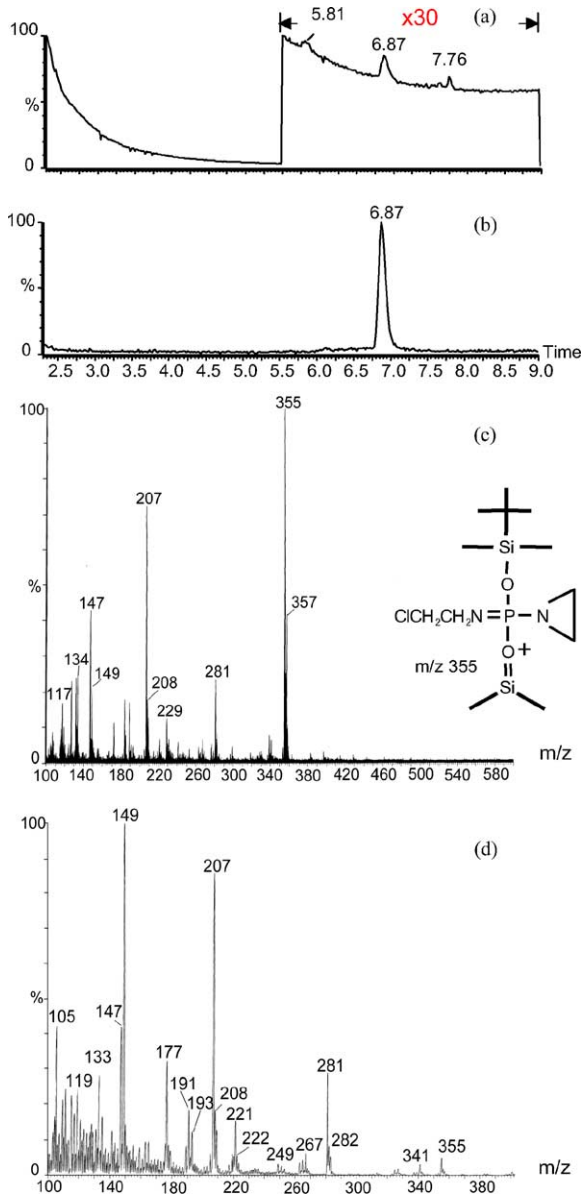

Fig. 2. Gas chromatography–mass spectrometry of TBDMS-derivatized IPM. (a) TIC from *m/z* 100–600; (b) selected ion chromatogram of *m/z* 355; (c) electron ionization mass spectrum corresponding to the peak at 6.87 min; (d) solvent blank showing background.

This coelution of an interfering background peak at *m/z* 355 was an unanticipated problem that degraded the quantitative aspect of IPM determinations. Thus, not only did the derivatization approach add an extra labor-intensive step, but it also presented additional difficulties such as the possibility for incomplete derivatization, and overlap with an interfering mass spectral background peak of variable intensity originating from column bleed. Moreover, even in more favorable situations where interfering mass spectral peaks are not present, it is not always reliable to use a fragment ion peak from electron ionization for quantification of the analyte because the yield of such fragment ions can be influenced to some degree by mass spectral conditions. Thus,

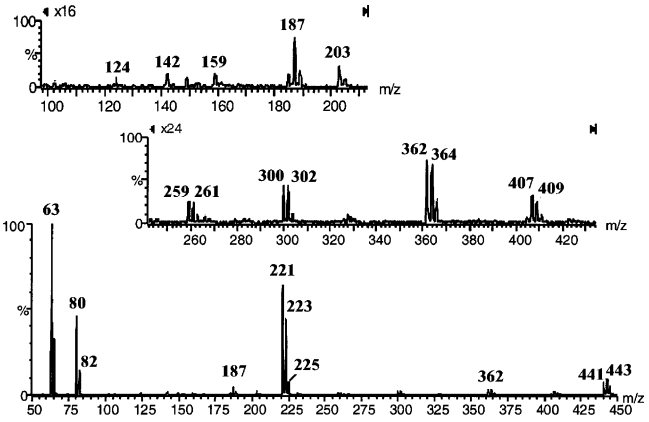

Fig. 3. Direct infusion mass spectrum of synthesized IPM. Top and middle traces are magnified traces of the regions from *m*/*z* 100 to 210 and *m*/*z* 240 to 430, respectively.

any such variability in the height of the peak at *m*/*z* 355 adds uncertainty to the determination. Because of these disadvantages, development of a direct analysis method (i.e., without derivatization) was undertaken.

3.2. HPLC analysis

In preliminary HPLC studies, it was revealed that IPM was rather unstable over time in various mobile phase solutions, as evidenced by the increasing number of peaks representing reaction products and the concomitant lower intensity of the IPM peak.

3.3. Direct MS and direct MS/MS analysis of IPM

The results obtained from direct MS analysis showed minimal detectable ions above *m*/*z* 450. Fig. 3 displays the ES mass spectrum of directly infused IPM from *m*/*z* 50 to 450. Protonated molecules (MH^+) of IPM appeared at *m*/*z* 221 along with M + 2 and M + 4 peaks at *m*/*z* 223 and 225, respectively, showing the typical isotopic distribution of molecules having two chlorine atoms. Protonated dimers of IPM appeared at *m*/*z* 441 (monoisotopic mass) along with the corresponding isotope peaks. In order to minimize the appearance of water clusters, the "cone" voltage in this experiment was set at 46 V. This condition resulted in a moderate level of "in-source" or "up-front" CID yielding strong signals corresponding to ions containing one chlorine at *m*/*z* 80 and 63, which can be assigned as $ClCH_2CH_2NH_3^+$ and $ClCH_2CH_2^+$, respectively; the low intensity peak at *m*/*z* 203 corresponds to the loss of H_2O. To aid in the assignment of other minor peaks, tandem mass spectrometry experiments were undertaken.

The MS/MS product ion spectrum of protonated IPM at *m*/*z* 221 is shown in Fig. 4a, revealing decomposition products at *m*/*z* 159, 142, 124, 106, 80, 63 and 44. The analogous product ion spectrum of protonated IPM molecules containing one ^{37}Cl atom (*m*/*z* 223, Fig. 4b), shows fragment ions at all of these same *m*/*z* values while yielding additional decomposition products corresponding to [M + 2] chlorine-containing peaks at *m*/*z* 161, 144, 126, 82, and 65. Thus, all CID fragments contain at least one chlorine atom except for those at 106 and 44. Assignments for all observed IPM decomposition products are given in Table 1. Many of these fragment ions observed by MS/MS analysis were also seen in the direct-infusion MS spectrum, suggesting that in-source decomposition of IPM was responsible for the production of these ions in Fig. 3. In the conventional mass spectrum, in-source fragmentation may be reduced by lowering the cone voltage; however, the water cluster ions concomitantly become significant, resulting

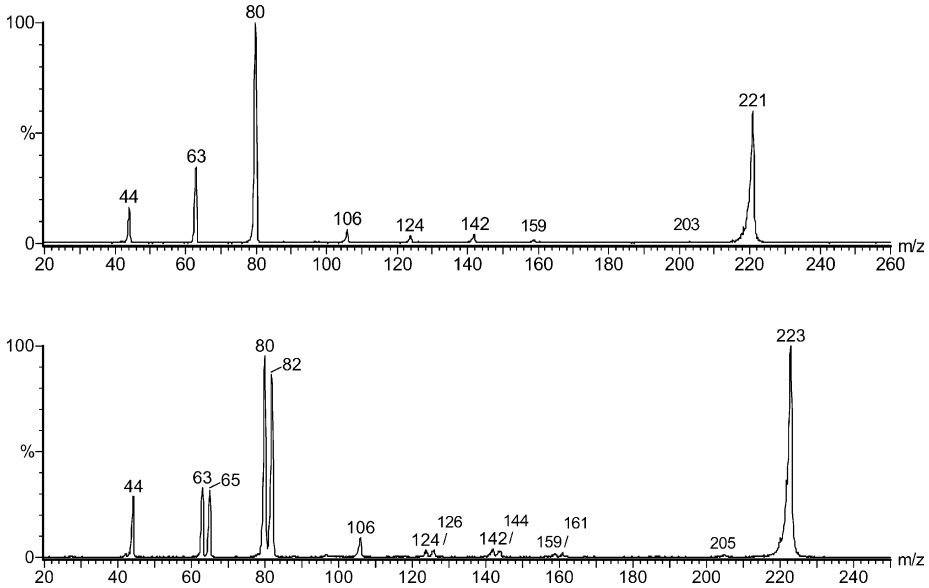

Fig. 4. Tandem mass spectrometry of IPM. (a) MS/MS product ion spectrum of MH^+ (*m*/*z* 221) precursor; (b) MS/MS product ion spectrum of [M + 2] precursor of MH^+ (*m*/*z* 223) that contains one ^{37}Cl.

Table 1
Assignments of CID fragments of protonated IPM (*m/z* 221) precursor

m/z	Assignment
44	
63	
80	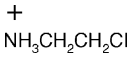
106	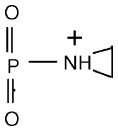
124	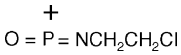
142	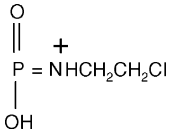
159	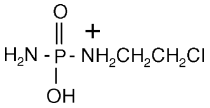
221	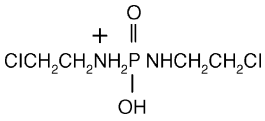

in a substantial reduction in signal levels of IPM and related peaks.

3.4. LC–MS analyses

A test run of LC–MS was conducted to monitor any ions in the *m/z* 50–450 range for 60 min to ensure total elution. Because no compounds were observed to elute after 40 min, in subsequent LC–MS runs, mass spectrometer scans acquired from *m/z* 50 to 450 were halted after 40 min. Fig. 5 shows the TIC along with relevant selected ion chromatograms. Three main peaks were observed at retention times of 3.5, 7.6 and 16.0 min. Other than the product appearing at 3.5 min (*m/z* 187, 189) and that appearing at 7.6 min (*m/z* 259, 261, 263, 265) the other detected ions observed in Fig. 3 appear at the identical retention time as that of IPM (16.0 min). Therefore, fragments at *m/z* 63, 80, and 203 (plus isotopes) assigned above, and ions at *m/z* 300 (assigned as $[IPM + NH_2CH_2CH_2Cl + H]^+$) and 362 (assigned as $[IPM + ClCH_2CH_2NHP(=O)=O + H]^+$) can all be designated (with their isotopes) as in-source fragments of either protonated IPM, or the protonated (noncovalent) dimer of IPM. The one remaining species at *m/z* 407 in Fig. 3, can be assigned as the protonated mixed dimer [IPM + unknown at 186 Da + H]$^+$; it does not appear in the LC–MS run because the component molecules were chromatographically separated from one another.

Fig. 6b, d and f shows the mass spectra corresponding to the peaks with retention times of 3.5, 7.6, and 16.0 min, respectively. There were no LC peaks observed after the elution of IPM. After thorough checking of all obtained mass spectral scans, only two significant contaminant compounds (appearing in protonated form at *m/z* 187 with neutral molecular weight 186 Da, and *m/z* 259 also in protonated form with neutral molecular weight 258 Da) were detected at retention times of 7.6 and 3.5 min, respectively. The *m/z* 187 product was suspected to be formed as a by-product during the manufacture of IPM, as it was not detectable as an impurity in the intermediate (phenyl ester of IPM) obtained prior to hydrogenation. Additionally, the abundance of *m/z* 187 did not increase after 1 h spent in the LC mobile phase. Direct infusion MS (Fig. 3) and LC–MS (Fig. 6d) show that *m/z* 187 contains one chlorine atom, while *m/z* 259 contains three chlorines (Fig. 6b), as revealed by the isotopic distributions.

3.5. LC–MS/MS analyses

On-line LC–MS/MS was performed on ions at *m/z* 187 (Fig. 6e), 189, 221 (Fig. 6g), 223, 259 (Fig. 6c), and 261 to obtain structural information pertaining to IPM, possible side products, and other possible contaminants.

3.5.1. Identification of impurity ions at m/z 187

The LC–MS/MS spectrum of *m/z* 187 (Fig. 6e) reveals several fragment ions (i.e., *m/z* 44, 63, 80, 142, and 159) observed in the MS/MS spectrum of protonated IPM (*m/z* 221), implying that this impurity contains certain structural features that are similar to IPM. In addition, other CID products are observed at *m/z* 29, 46, and 108. These latter fragments are all consistent with the presence of an ethyl group replacing a chloroethyl group at one of the amino nitrogens. All CID products are assigned in Table 2. The contaminant ion observed at *m/z* 187 appears at 34 *m/z* units less than IPM, and is thus assigned as the protonated (MH^+) form of *N*-(2-chloroethyl)-*N*′-ethylphosphorodiamidic acid (MW = 186 Da), very likely resulting from the loss of HCl during synthesis, followed by hydrogenation as shown in Scheme 1. CID of the (M + 2) peak at *m/z* 189 clearly reveals additional product ions at *m/z* 65 and 82, indicative of the presence of ^{37}Cl in these fragments. *N*-(2-Chloroethyl)-*N*′-ethylphosphorodiamidic acid (that we are calling "MC-IPM" for monochloro-IPM), was subsequently synthesized and characterized by NMR. After spiking it into an IPM stock solution, LC–MS analysis showed that the peak at *m/z* 187 increased dramatically without significantly altering the retention time or the peak shape. In addition, MS/MS of the protonated molecule of synthesized *N*-(2-chloroethyl)-*N*′-ethylphosphorodiamidic acid was also performed, and it gave the identical decomposition pattern as the MS/MS product ion spectrum of *m/z* 187 impurities

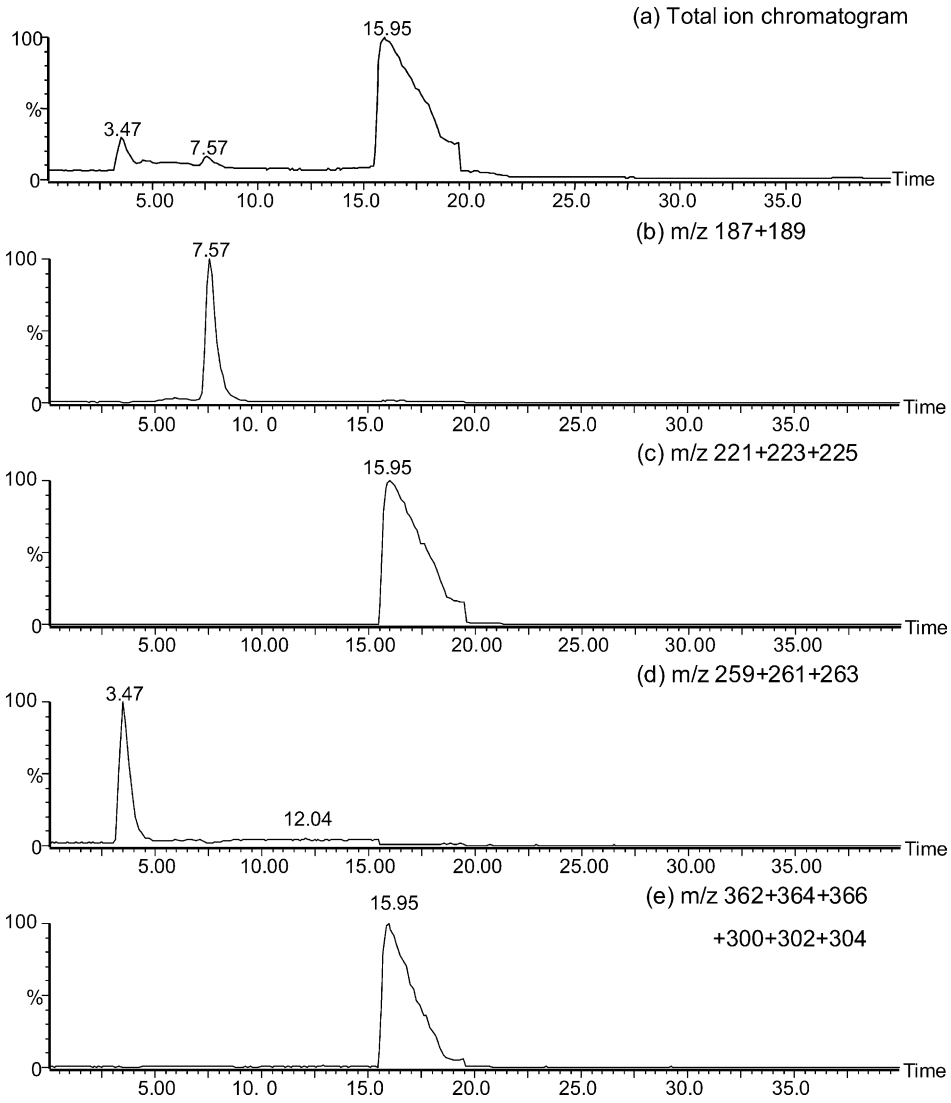

Fig. 5. TIC and selected ion chromatograms of synthesized IPM. By monitoring retention times associated with appearing ions, all species observed in the conventional mass spectrum (Fig. 3), except those giving peaks at *m*/*z* 187, 259, and 407 (see text) are deduced to be in-source CID fragments of either IPM or the protonated dimer of IPM.

found in synthesized IPM. During the hydrogenation step of the IPM synthesis, aliquots were removed at various time intervals. The impurity peak was observed to increase in intensity as the hydrogenation step progressed. The above combined evidence allows the positive identification of *N*-(2-chloroethyl)-*N*′-ethylphosphorodiamidic acid as the principal impurity.

To our knowledge, this monochlorinated derivative of IPM, i.e., MC-IPM, has not been reported in the literature. Millis et al. [11] reported that IPM forms a "relatively stable" aziridine derivative, IPM-aziridine (MW = 185), when IPM was incubated for ∼30 min in aqueous solution between pH 2 and 10. However, although we are postulating IPM-aziridine as an intermediate to MC-IPM formation (the penultimate molecule that undergoes hydrogenation in Scheme 1), IPM-aziridine was not observed in our studies by HPLC-UV or by LC–MS.

3.5.2. Identification of ions at m/z 259

In certain trials, ions at *m*/*z* 259 were observed in the LC–MS chromatogram at 3.5 min (see Fig. 5a,5d and 6b,6c). It was later established that this peak only appeared when IPM was allowed to stand in the perchloric acid mobile phase for at least 1 h prior to injection. Thus, the ion at *m*/*z* 259 corresponds to a compound that is not initially present in synthesized IPM. The compound contains three chlorine atoms, as revealed by the isotopic distribution (Figs. 3 and 6b). The LC–MS/MS spectrum of this compound (Fig. 6c) yielded only three discernable fragment peaks (*m*/*z* 63, 80 and 159). The one major peak at *m*/*z* 80 and the minor peak at *m*/*z* 63 were indicative of a $NHCH_2CH_2Cl$ moiety in both

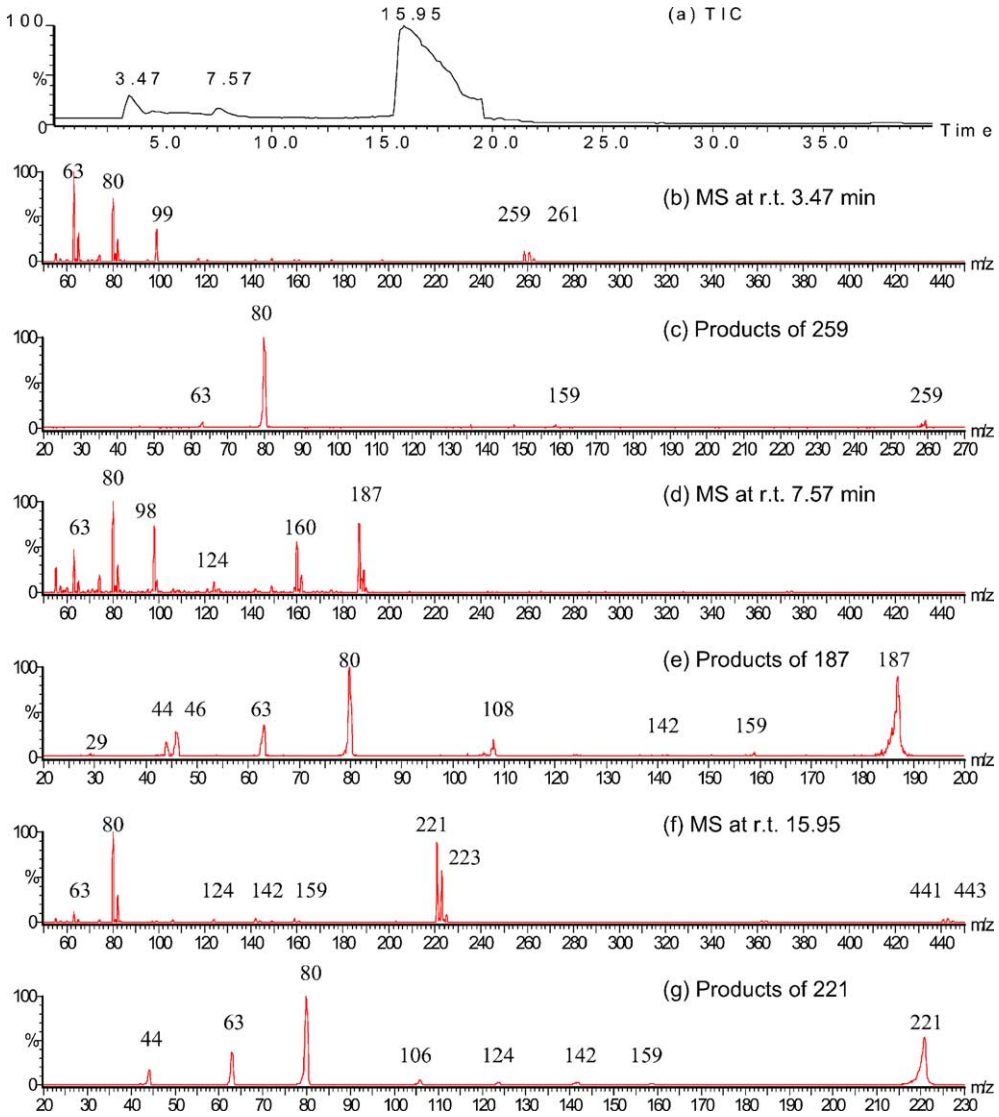

Fig. 6. LC–MS and LC–MS/MS decomposition spectra of synthesized IPM (retention time 16.0 min) and two contaminant peaks with retention times of 3.5 and 7.6 min.

IPM and MC-IPM (see Tables 1 and 2), so it is inferred that this moiety remains intact in the *m/z* 259 product. The LC–MS/MS spectrum of the [M+2] peak at *m/z* 261 yielded the same three peaks, plus additional peaks at *m/z* 65, 82 and 161. The 100 Da neutral that is lost from both *m/z* 259 and 261 is proposed to be $HO^{35}ClO_3$. From these data, we propose that *m/z* 259 represents the protonated form of a compound having a molecular formula of $C_2H_6N_2O_4PCl_3$ (proposed structure given in Fig. 7) that results from a reaction of IPM with perchloric acid (and ubiquitous Cl^-) in the mobile phase.

3.5.3. LC–MS detection limit and purity of IPM

The LC–MS detection limit has been estimated as ~13.5 ng, or ~2.7 ng/μl using 5.0 μl injections. Several batches of IPM have been analyzed. Employing the simplifying assumption that the ionization efficiencies of *N*-(2-chloroethyl)-*N′*-ethylphosphorodiamidic acid and IPM are approximately equal, the purity of IPM is estimated to be in the range of 95–98%.

3.5.4. Plasma study

In order to test the ability to detect IPM and metabolites in a genuine blood extract, a plasma sample was prepared by centrifuging human blood for 5 min at 3000 rpm. The obtained plasma sample was spiked with IPM to a final concentration of 100 ng/μl. Fig. 8 shows the TIC and the summed selected ion chromatogram of *m/z* 221 and 223. The peak corresponding to IPM appears at 18.6 min, representing a shift in retention time (increased retention) of about 2.6 min relative to the IPM peak appearing in the chromatogram shown in Fig. 6. The shift in retention time is

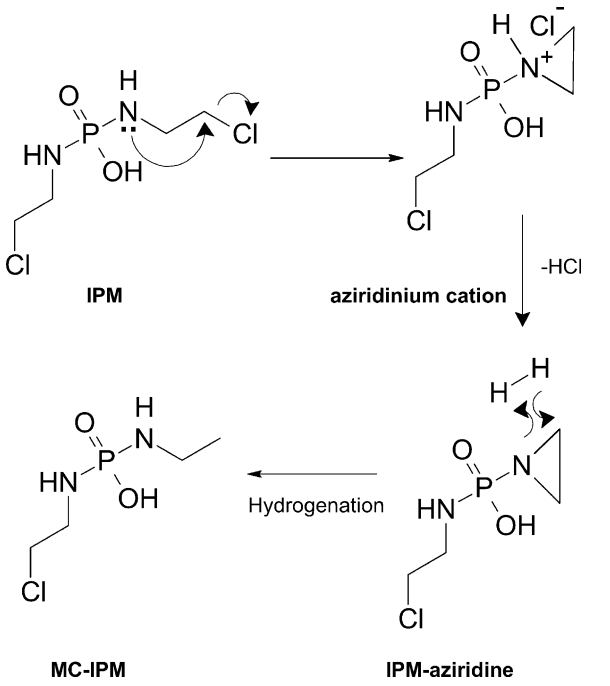

Scheme 1. Proposed mechanism of *N*-(2-chloroethyl)-*N′*-ethylphosphorodiamidic acid (monochloro-IPM, MC-IPM) formation.

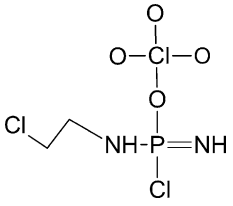

Fig. 7. Proposed structure of 258 Da neutral molecule appearing in electrospray mass spectra in protonated form at *m*/*z* 259. The *m*/*z* 259 ion can be detected only after IPM has been exposed to dilute perchloric acid for at least 1 h.

likely attributable to a combination of matrix effects from the plasma, and column overloading in the prior standard run. The presence of interfering background species largely masks the IPM peak in the TIC.

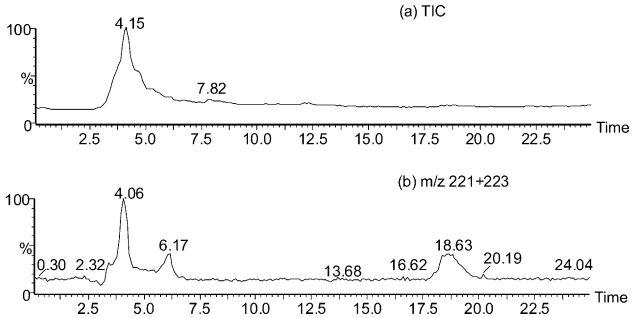

Fig. 8. (a) TIC (*m*/*z* 50–450) of 100 ng/μl IPM spiked in human plasma. No clear IPM peak is observed. (b) Selected ion chromatogram at *m*/*z* 221and 223. The IPM peak appears at 18.6 min. However, the peaks that appear at 4.1 and 6.2 min are unknown components in plasma yielding ions at *m*/*z* 221 (no 223).

Table 2
Assignments of CID fragments of *m*/*z* 187 precursor deduced to be protonated MC-IPM

m/*z*	Assignment
29	$CH_2CH_3^+$
44	
46	$NH_3CH_2CH_3^+$
63	$CH_2CH_2Cl^+$
80	$NH_3CH_2CH_2Cl^+$
108	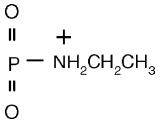
142	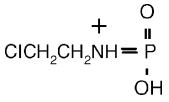
159	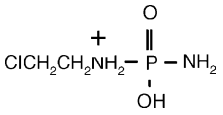
187	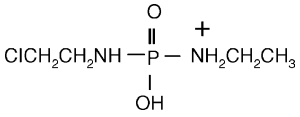

4. Conclusion

A LC–MS/MS method has been developed to rigorously analyze in-house synthesized IPM. The main impurity, present at 2–5%, has been conclusively identified as *N*-(2-chloroethyl)-*N′*-ethylphosphorodiamidic acid (MC-IPM). In separate studies, this impurity has been established to be nontoxic in animal tests. Moreover, its presence can be reduced by recrystallizing the final IPM product in cold acetone (IPM has a lower solubility). A second detected impurity did not originate during IPM synthesis, but rather, it was found to be the product of reaction of IPM with the perchloric acid mobile phase used for liquid chromatography. A study of IPM-spiked plasma has established the ability to detect IPM in the presence of a large background of blood constituents. This latter demonstration bodes well for the future use of the LC–MS/MS method in investigations of the pharmacokinetics of IPM in plasma.

Acknowledgements

This research is supported in part by grant #R44 CA83552 from the NCI/SBIR program and in part by grant

#LEQSF(2001-04)-RD-B-11 from the Louisiana Board of Regents Support Fund.

References

[1] R.F. Struck, D.J. Dykes, T.H. Corbett, W.J. Suling, M.W. Trader, Br. J. Cancer 47 (1983) 15.
[2] M. Zalupski, L.H. Baker, J. Natl. Cancer Inst. 80 (1988) 556.
[3] W.P. Brade, K. Herdrich, M. Varini, Cancer Treatment Rev. 12 (1985) 1.
[4] J.J. Costanzi, L.R. Morgan, J. Hokanson, Semin. Oncol. 9 (1982) 61.
[5] O.M. Friedman, A.M. Seligman, J. Am. Chem. Soc. 76 (1954) 655.
[6] E. Watson, P. Dea, K.K. Chan, J. Pharmaceutic. Sci. 74 (1985) 1283.
[7] J. Cohen, J. Jusko, W.J. Yao, Br. J. Pharmacol. 43 (1971) 677.
[8] F.D. Juma, J.J. Rodgers, J.R. Trounce, Br. J. Pharmacol. 10 (1980) 327.
[9] J.J. Zheng, K.K. Chan, F. Muggia, Cancer Chemother. Pharmacol. 33 (1994) 391.
[10] T.P. Mawhinney, R.S.R. Robinett, A. Atalay, M.A. Madson, J. Chromatogr. 358 (1986) 231.
[11] K.K. Millis, M.E. Colvin, E.M. Shulman-Roskes, S.M. Ludeman, O.M. Colvin, M.P. Gamcsik, J. Med. Chem. 38 (1995) 2166.
[12] N. Germann, S. Urien, A.H. Rodgers, L.R. Morgan, M. Ratterree, R.F. Struck, W.R. Waud, D.G. Serota, G. Bastian, 14th EORTC/NCI/AACR Conference, Frankfurt, Germany, November 2002.